

High fidelity parameter scans in a 5 Hz plasma wakefield accelerator

*Contact: m.streeter@lancaster.ac.uk

S. J. D. Dann, J. D. E. Scott, M. J. V. Streeter*
*The Cockcroft Institute, Keckwick Lane,
Daresbury, WA4 4AD, UK*

**J. Hah, K. Krushelnick, J. Nees,
A. G. R. Thomas**
*Center for Ultrafast Optical Science, University of
Michigan, Ann Arbor, Michigan 48109-2099, USA*

J. Osterhoff, P. Pourmoussavi
*Deutsches Elektronen-Synchrotron DESY,
Notkestr. 85, 22607 Hamburg, Germany*

C. Baird, C. D. Murphy
*Department of Physics, University of York, Heslington,
York YO10 5DD, UK*

M. Krishnamurthy, S. Tata
*Tata Institute of Fundamental Research,
Homi Bhabha Road, Colaba, India*

**N. Bourgeois, O. Chekhlov, C. D. Gregory,
S. J. Hawkes, C. J. Hooker, V. Marshall,
B. Parry, P. P. Rajeev, E. Springate,
D. R. Symes, Y. Tang, C. Thornton**
*Central Laser Facility, Rutherford Appleton Laboratory,
Didcot OX11 0QX, UK*

**S. Eardley, J.-N. Gruse, S. P. D. Mangles,
Z. Najmudin, S. Rozario, R. A. Smith**
*Physics Department, Imperial College London,
London, SW7 2AZ, UK*

S. V. Rahul
*TIFR Centre for Interdisciplinary Sciences,
Hyderabad 500 107, India*

D. Hazra
*Laser Plasma Section, Raja Ramanna Centre for
Advanced Technology, Indore 452013, India*

Abstract

We present experimental data showing the beneficial effects of performing parameter scans with a high repetition rate laser. The transmitted laser and electron beam generated in a laser-driven plasma wakefield accelerator are clearly observed to depend on the gas jet backing pressure. The spectral properties of these beams are seen to be smooth functions of the input parameters, when averaging over a set 49 shots for each value and employing gradual changes in pressure. This allows for detailed examination of the interaction physics, and can better reveal threshold behaviour and highly localised optima. Extending high-repetition rate operation to higher power laser systems is expected to yield great benefits in performance, and will enable a range of new applications.

1 Introduction

The Central Laser Facility has a rich history in laser driven plasma wakefield experiments starting with landmark work by Modena *et al.* [1]. In that paper, the authors describe pioneering work using the newly commissioned chirped-pulse amplified beamline of the VULCAN laser. With ps long pulses and a peak intensity of $5 \times 10^{18} \text{ Wcm}^{-2}$ they were able to drive strong plasma waves, enhanced by the self-modulation of the driving laser pulse, that resulted in wavebreaking and acceleration of trapped electrons up to 44 MeV. Subsequent experiments greatly developed these concepts, but a major breakthrough was enabled by the ASTRA laser, which was capable of multi-TW peak powers with

a pulse duration of just $\tau_L = 40$ fs. This enabled experimenters to demonstrate plasma wave generation in the ‘forced’ LWFA regime, i.e. $\tau_L \lesssim 2\pi/\omega_p$ where $\omega_p = \sqrt{n_e e^2 / (m_e \epsilon_0)}$ is the plasma frequency for a plasma with electron density n_e . In this regime, wavebreaking can occur in the first plasma period, resulting in a short burst of injection and subsequent acceleration of narrow energy spread electron beams. The highly-cited paper by Mangles *et al.* [2], describes an experiment using the Astra laser which obtained beams of electrons with energies up to 80 MeV, and 3% energy spreads. This work demonstrated the potential to produce controlled electron beams with narrow energy spreads and led to international projects aiming at applying LWFA accelerated electron beams to future light sources [3, 4, 5, 6] and colliders [7].

More immediate applications have emerged in using compact radiation generation mechanisms. Betatron oscillations of the electrons inside an LWFA, can lead to the generation of a bright X-ray beam [8]. The strong focusing forces of the plasma wakefield causes electrons, with an energy given by $\gamma m_e c^2$, to oscillate with the characteristic betatron frequency $\omega_\beta = \omega_p / \sqrt{2\gamma}$. The emitted radiation is then typically synchrotron-like with a characteristic energy $\hbar\omega = 3\gamma^2 \hbar\omega_\beta$. The small source size and high peak brightness of these X-rays, enables single-shot phase contrast imaging [9, 10] and even full 3D tomographic reconstruction with the use of 100s of shots [11, 12]. Compact gamma radiation sources have also been produced through inverse Compton scattering [13] and bremsstrahlung [14]. The co-location of a high brightness X-ray/gamma source with a high power

laser system provides an experimental platform that is otherwise only achievable with very expensive and large-footprint combination of radio-frequency based accelerators and high power lasers. Several recent experiments have leveraged this capability at the Central Laser Facility to perform studies of laser driven shocks [15] and quantum radiation reaction [16, 17]. The vast majority of these world leading experiments would benefit greatly from being able to shoot at an increased repetition rate. Not only would it be possible to take more data and gain higher statistical significance in the results, it would also allow for entirely different modes of operation and enable applications that are not currently viable at lower repetition rates.

Recent experiments using the Gemini 5 Hz 15 TW laser in TA2, have demonstrated the ability to control high-intensity laser-plasma interactions with active-feedback techniques to enhance generated X-ray [18] and electron beam [19] properties. Operating such interactions at high repetition rate also allows for huge numbers of shots to be taken over a wide range of experimental parameters. These parameter scans produce orders of magnitude more data than a single-shot approach, enabling high precision examinations of highly-nonlinear and threshold behaviours. In addition, by averaging over multiple shots it is possible to greatly reduce the effect of shot-to-shot variations and reveal the underlying behaviour with far greater clarity. Here, we report on results obtained from the first sustained 5 Hz LWFA campaign in Astra Gemini TA2.

2 Experiment

The experiment was set up in the Gemini TA2 target chamber as shown in fig. 1. Laser pulses containing 450 mJ at a central wavelength of 800 nm were focused with a 1 m focal length parabolic mirror, giving an effective f -number of 16.7 and FWHM spot diameter of $20 \mu\text{m}$. The pulse length at optimal compression was $34 \pm 2 \text{ fs}$, providing a peak vacuum intensity $I_0 \approx 1.5 \times 10^{18} \text{ Wcm}^{-2}$ and peak normalised vector potential $a_0 \approx 0.9$. A custom-built (by the CLF) deformable mirror with 55 actuators and a high reflectivity dielectric coating was used to optimise the laser wavefront, and an acoustic-optical programmable dispersive filter (DAZZLER) was used to control the spectral phase of the compressed pulse. This allowed the temporal profile of the laser pulse to be varied over a wide range. The laser was capable of firing single isolated shots, or bursts of 49 shots at 5 Hz.

A pressurised methane gas reservoir (0–40 bar) was connected to a 3 mm gas nozzle via a pulsed solenoid valve. When triggered, the gas expanded from the nozzle outlet and rapidly cooled, forming a mixed medium of molecular and clustered methane, into which the laser was focused. A differentially pumped chamber enclosed the gas jet, in order to maintain a pressure below

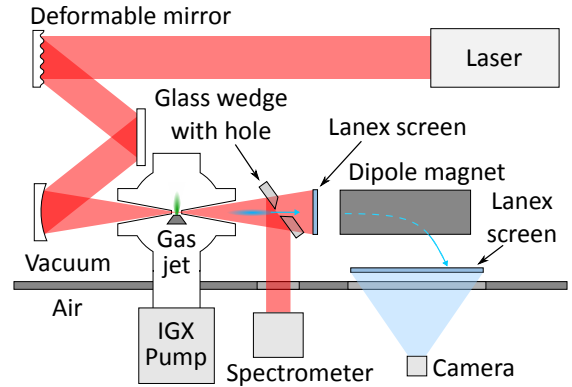


Figure 1: A schematic of the experimental setup. The laser is focused into a pulsed methane gas jet inside a differentially pumped inner chamber. Exit mode light and accelerated electrons are diagnosed by optical and magnetic spectrometers respectively.

10^{-3} mbar in the target and laser compressor chambers. Inlet and outlet apertures were used to allow the laser pulse to enter the internal chamber, and for the laser and generated secondary radiation to exit. The transmitted laser pulse, after exiting the plasma, was partially reflected by a glass plate, with an on-axis hole to allow propagation of the electron and X-ray beams. The partial reflection was directed to a spectrometer to measure the transmitted laser spectrum over the wavelength range 360–920 nm. The electron beam entered a magnetic dipole field, inside a radiation shielded chamber, which dispersed the beam by energy onto a Lanex scintillator screen. An optical camera imaged the emission from the screen, to provide a measurement of the electron beam spectrum.

Figure 2 shows the transmitted laser spectrum as a function of the backing pressure to the gas nozzle. In the first instance (fig. 2a), the laser was optimally compressed and we performed a pressure scan taking a single shot at each pressure. By using 165 shots, it was possible to see the overall trend of the spectral shifts of the laser pulse as the backing pressure was changed, despite considerable shot-to-shot variation (25% RMS). In the second instance (fig. 2b), the laser pulse was set to a previously determined optimal temporal shape for electron acceleration [19], and 49 shots were taken at each pressure. A marked difference in behaviour is observed, with a considerable reduction in blueshift of the driving laser pulse, and enhanced redshift. The reduced blueshift suggests a reduction in ionization of the methane by the peak intensity of the laser pulse. The increased redshift that occurs for $P > 3$ bar is symptomatic of driving a high amplitude plasma wave, which depletes the leading edge of the pulse, causing a reduction in photon energy $\hbar\omega$. A comparison of the two data sets in fig. 2 also shows that the quality of the data is greatly increased by av-

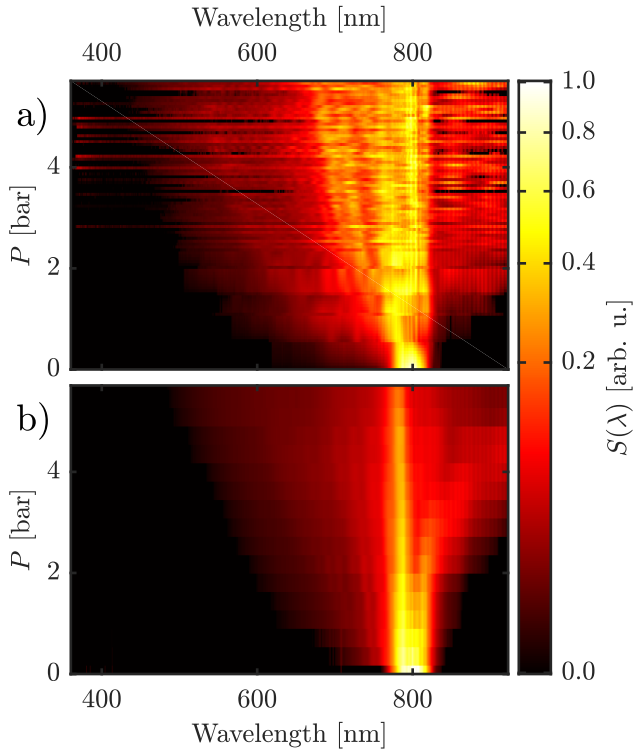


Figure 2: Transmitted laser spectra for a) the fully compressed laser pulse and b) a laser pulse shape which was optimised for electron beam generation, both as functions of backing pressure. For a) each row is a single shot, whereas in b) each row is the average of 49 shots. Note the non-linear colour mapping to make the low intensity regions visible.

eraging over multiple shots. The high-frequency noise, visible in fig. 2a, is all but removed, leaving only the features which consistently appear for the same nominal input parameters. The underlying trend in the spectral modification of the driving laser pulse by the plasma interaction becomes more visible, and features at relatively low intensities become detectable.

Figure 3 shows the spectra of the detected electron beams for the same shots as fig. 2. The random variations are even more pronounced for the electron spectra data made of single shots with the shortest compressed pulse, as seen in fig. 3a. When averaging over 49 shots using the optimally shaped pulse, as seen in fig. 3b, the injection threshold pressure is clearly observable as a significant increase in charge around $P = 5$ bar. Shot-to-shot fluctuations obscure much of the general behaviour when taking only one shot per pressure value. In addition the optimally shaped pulse causes significantly more charge to be injected than the shortest compressed pulse does. During the optimisation process, the injected charge doubled; the more extreme change seen here might be caused by additional fine-tuning of the accelerator, which took place after collecting the data

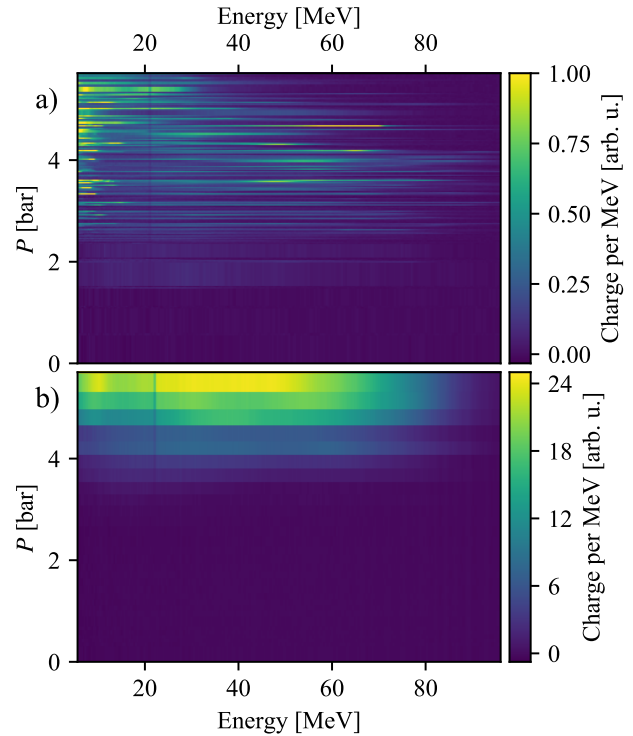


Figure 3: Electron spectra for a) the fully compressed laser pulse and b) a laser pulse shape which was optimised for electron beam generation, both as functions of backing pressure. For a) each row is a single shot, whereas in b) each row is the average of 49 shots.

shown in fig. 3a.

Figure 4 shows the electron and transmitted laser spectra for a full parameter scan of the backing pressure to the gas nozzle. Each row is averaged over 49 shots, allowing for clear observation of the experimental behaviour. The highest energy electrons (fig. 4a) are observed at 5 bar, while the maximum electron spectral intensity and a reduced energy spread is observed at 6.5 bar. Significant frequency shifting of the driving laser pulse was observed at low densities (fig. 4b), below the threshold pressure for observation of an electron beam. Strong redshifting has been observed to correlate with pulse self-compression, leading to an increase in the a_0 of the laser pulse. This indicates that significant pulse evolution is required in order to trigger trapping of plasma electrons into the LWFA [20]. Further increasing the backing pressure beyond these optimal values leads to a decrease of observed electron beam energy. This behaviour is consistent with the typical dephasing limited energy [21] which scales with plasma density as $W_{\max} \propto n_e^{-1}$ [22].

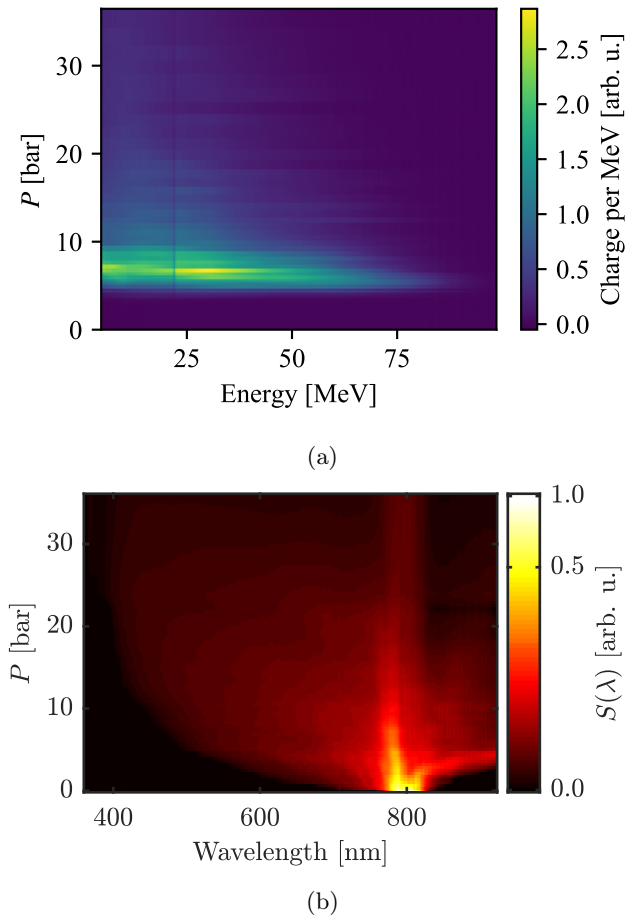


Figure 4: a) Electron spectrum and b) transmitted laser spectra as functions of backing pressure.

3 Conclusion

These results demonstrate the increased fidelity one can obtain in parameter scans using high repetition rate lasers. This is commonplace in lower intensity kHz laser experiments, but only recently has this been applied to relativistic intensities. With a high-fidelity scan of the target backing pressure we were able to observe a clear threshold for the internal injection and acceleration of relativistic electron beams. A narrow window of optimal pressure was discovered which optimised both the accelerated charge, and the resultant spectrum. Such fine features in the vast parameter space would easily be missed without the benefit of a high precision parameter scan and multi-shot averaging to reduce the scatter in the data.

There is a clear requirement to move to high repetition rates in order to enable many potential applications of LWFA. With this experiment we have started to address the technical challenges that arise from this new mode of operation. The total number of shots generating ~ 50 MeV electron beams in this experiment was estimated at 100,000, (approximately 6 hours of contin-

uous shooting). By contrast, Gemini TA3 recently fired its 200,000th shot, in its 10th year of operation. With the excellent results emerging from Gemini from many different types of experiments, the benefits of increasing repetition rate capabilities, of both the laser and the experimental apparatus, are abundantly obvious.

Acknowledgements

We acknowledge funding from STFC (grant numbers ST/P002056/1 and ST/P002021/1), and the EuroNNAc, Newton-Bhabha and Helmholtz ARD programs. SE is supported by an AWE CASE award. JH, JN, KK and AT acknowledge funding from the NSF grant 1535628 and DOE grant DE-SC0016804. The authors also thank the staff of the Central Laser Facility for their expertise and their essential contributions to this work.

References

- [1] A. Modena et al. Electron acceleration from the breaking of relativistic plasma waves. *Nature* **377**, (Oct. 1995), pp. 606–608. URL: <http://dx.doi.org/10.1038/377606a0>.
- [2] S. P. D. Mangles et al. Monoenergetic beams of relativistic electrons from intense laser-plasma interactions. *Nature* **431**, (2004), pp. 535–538. URL: <https://www.nature.com/articles/nature02939>.
- [3] Carl B. Schroeder et al. “Free-electron laser driven by the LBNL laser-plasma accelerator”. *AIP Conference Proceedings*. Vol. 1086. 1. AIP, Jan. 2009, pp. 637–642. URL: <http://aip.scitation.org/doi/abs/10.1063/1.3080982>.
- [4] S M Wiggins et al. High quality electron beams from a laser wakefield accelerator. *Plasma Physics and Controlled Fusion* **52**, 12 (Dec. 2010), p. 124032. URL: <http://iopscience.iop.org/article/10.1088/0741-3335/52/12/124032/meta>.
- [5] Andrea R. Rossi et al. The External-Injection experiment at the SPARC LAB facility. *Nuclear Instruments and Methods in Physics Research Section A: Accelerators, Spectrometers, Detectors and Associated Equipment* **740**, (Mar. 2014), pp. 60–66. URL: <http://linkinghub.elsevier.com/retrieve/pii/S016890021301454X>.
- [6] M E Couprie et al. “The LUNEX5 Project in France”. *Springer Proceedings in Physics*. Vol. 147. 7. IOP Publishing, Mar. 2014, pp. 55–62. URL: http://link.springer.com/10.1007/978-3-319-00696-3_10.
- [7] C. B. Schroeder et al. Physics considerations for laser-plasma linear colliders. *Physical Review Special Topics - Accelerators and Beams* **13**, 10 (Oct. 2010), p. 101301. URL: <http://link.aps.org/doi/10.1103/PhysRevSTAB.13.101301>.
- [8] Antoine Rousse et al. Production of a keV X-Ray Beam from Synchrotron Radiation in Relativistic Laser-Plasma Interaction. *Physical Review Letters* **93**, 13 (Sept. 2004), p. 135005. URL: <http://link.aps.org/doi/10.1103/PhysRevLett.93.135005>.
- [9] S. Kneip et al. X-ray phase contrast imaging of biological specimens with femtosecond pulses of betatron radiation from a compact laser plasma wakefield accelerator. *Applied Physics Letters* **99**, 9 (Aug. 2011), p. 093701. URL: <http://aip.scitation.org/doi/10.1063/1.3627216>.

- [10] S. Fourmaux et al. Single shot phase contrast imaging using laser-produced Betatron x-ray beams. *Optics Letters* **36**, 13 (July 2011), p. 2426. URL: <https://www.osapublishing.org/abstract.cfm?URI=ol-36-13-2426>.
- [11] J. Wenz et al. Quantitative X-ray phase-contrast microtomography from a compact laser-driven betatron source. *Nature Communications* **6**, 1 (Dec. 2015), p. 7568. URL: <http://www.nature.com/articles/ncomms8568>.
- [12] J M Cole et al. Tomography of human trabecular bone with a laser-wakefield driven x-ray source. *Plasma Physics and Controlled Fusion* **58**, 1 (Jan. 2016), p. 014008. URL: <http://iopscience.iop.org/article/10.1088/0741-3335/58/1/014008>.
- [13] K. Ta Phuoc et al. All-optical Compton gamma-ray source. *Nature Photonics* **6**, 5 (May 2012), pp. 308–311. URL: <http://www.nature.com/articles/nphoton.2012.82>.
- [14] R. D. Edwards et al. Characterization of a gamma-ray source based on a laser-plasma accelerator with applications to radiography. *Applied Physics Letters* **80**, 12 (Mar. 2002), pp. 2129–2131. URL: <http://aip.scitation.org/doi/10.1063/1.1464221>.
- [15] J. C. Wood et al. Ultrafast Imaging of Laser Driven Shock Waves using Betatron X-rays from a Laser Wakefield Accelerator. *arXiv.org* (Feb. 2018). URL: <http://arxiv.org/abs/1802.02119>.
- [16] J. M. Cole et al. Experimental Evidence of Radiation Reaction in the Collision of a High-Intensity Laser Pulse with a Laser-Wakefield Accelerated Electron Beam. *Physical Review X* **8**, 1 (Feb. 2018), p. 011020. URL: <https://link.aps.org/doi/10.1103/PhysRevX.8.011020>.
- [17] K. Poder et al. Evidence of strong radiation reaction in the field of an ultra-intense laser. *arXiv.org* (Sept. 2017). URL: <http://arxiv.org/abs/1709.01861>.
- [18] M. J. V. Streeter et al. Temporal feedback control of high-intensity laser pulses to optimize ultrafast heating of atomic clusters. *arXiv.org* (Apr. 2018). URL: <http://arxiv.org/abs/1804.07488>.
- [19] S. J. D. Dam et al. Laser wakefield acceleration with active feedback at 5 Hz. *In preparation for submission* (2018).
- [20] M. J. V. Streeter et al. Observation of power amplification in a self-injecting laser wakefield accelerator. *arXiv.org* (Oct. 2017). URL: <http://arxiv.org/abs/1710.05337>.
- [21] M. S. Bloom et al. Bright X-ray radiation from plasma bubbles in an evolving laser wakefield accelerator. *arXiv.org* (Oct. 2017). URL: <https://arxiv.org/abs/1710.05740>.
- [22] W. Lu et al. Generating multi-GeV electron bunches using single stage laser wakefield acceleration in a 3D nonlinear regime. *Physical Review Special Topics - Accelerators and Beams* **10**, 6 (June 2007), p. 061301. URL: <http://link.aps.org/doi/10.1103/PhysRevSTAB.10.061301>.